Counting and Sequential Information Processing in Mechanical Metamaterials

Lennard J. Kwakernaak and Martin van Hecke
Huygens-Kamerlingh Onnes Laboratory, Universiteit Leiden, PO Box 9504, 2300 RA Leiden, Netherlands and AMOLF, Science Park 104, 1098 XG Amsterdam, Netherlands

(Received 15 February 2023; accepted 30 May 2023; published 30 June 2023)

Materials with an irreversible response to cyclic driving exhibit an evolving internal state which, in principle, encodes information on the driving history. Here we realize irreversible metamaterials that count mechanical driving cycles and store the result into easily interpretable internal states. We extend these designs to aperiodic metamaterials that are sensitive to the order of different driving magnitudes, and realize "lock and key" metamaterials that only reach a specific state for a given target driving sequence. Our metamaterials are robust, scalable, and extendable, give insight into the transient memories of complex media, and open new routes towards smart sensing, soft robotics, and mechanical information processing.

DOI: 10.1103/PhysRevLett.130.268204

Counting a series of signals is an elementary process that can be materialized in simple electronic or neural networks [1]. Even the Venus flytrap can count, as it only snaps shut when touched twice, despite not having a brain [2]. While the ability to count is not commonly associated with materials, certain complex materials, from crumpled sheets to amorphous media, can exhibit memory effects where the state depends on the driving history [3,4]. Under cyclic driving, their response then may feature subharmonic behavior [5–12] or, as was recently shown, a transient memory where the system only settles in a periodic response after $\tau > 0$ driving cycles [13–15]. Multiple transient memories occur when the material encodes the number of driving cycles of distinct magnitudes [16,17]. Materials that exhibit (multiple) transient memories can thus be regarded as counting.

So far, transient memories have been observed in disordered media. Disorder produces scatter in the critical driving thresholds that make the system evolve along a sequence of transient states, potentially leading to more complex memory effects. Hence, "counting" materials with controlled transients and thresholds can provide insight into (multiple) transient memory effects. In addition, they could simplify the design of soft robotics and intelligent sensors, and open a route towards sequential information processing.

Here we introduce a general platform for metamaterials [18] that count mechanical compression cycles. Its unit cells feature a memory beam (m-beam) that is either buckled left or right, which we represent with a binary value $s_i = 0$ or 1 [19] [Fig. 1(a)]. The unit cells are designed to interact with their neighbors such that under cyclic compression any unit cell in the 1 state copies this state to its right neighbor [Figs. 1(b) and 1(c)]. This leads to a mechanically clocked wave where the "1" state advances rightward, one unit cell per compression cycle. Hence, the collective state, $S := \{s_1, s_2, \ldots\}$, evolves like in a cellular automaton [20], with repeated cyclical compression yielding simple predictable pathways. Moreover, they provide a disorder-free, controllable materialization of transient memory. By combining such beam counters in aggregate metamaterials, we realize the detection of compression cycles of multiple amplitudes, tantamount to multiple transient memories. Finally, heterogeneous counters exhibit complex memory effects where the transient time depends on the driving magnitude and the response becomes driving-sequence dependent. Together, our metamaterials establish a general platform for realizing targeted multistep pathways in metamaterials and open a route towards sequential information processing *in materia* [21–23].

Unit cell and cyclic driving.—We aim to realize metamaterials where state 1 spreads to the right when the compressive strain ε is cycled between ε_m and ε_M (Fig. 1). We note that in contrast to recent metamaterials which exhibit sequential shape changes under monotonic driving [24–28], we require a sequential response under cyclic driving. This necessitates unit cells that memorize their previous state, interact with their neighbors, and break left-right symmetry. We satisfy these requirements with unit cells i containing two beams [Fig. 1(b)]. The slender m-beams encode states $s_i = 0$ or 1 in their left or right buckled configurations. We choose ε_m larger than their buckling strain so they retain their state. The thicker and nontrivially shaped a-beams facilitate interactions between the m-beams, and buckle at a strain larger than ε_m but smaller than ε_M.

The detailed design involves a careful choice of the symmetry breaking beam shapes and their spacings. First, weakly symmetry breaking rounded corners at the ends of the m-beams controls their buckling into a desired initial configuration $S = \{100\ldots\}$—this does not appreciably modify the evolution of the sample during compression

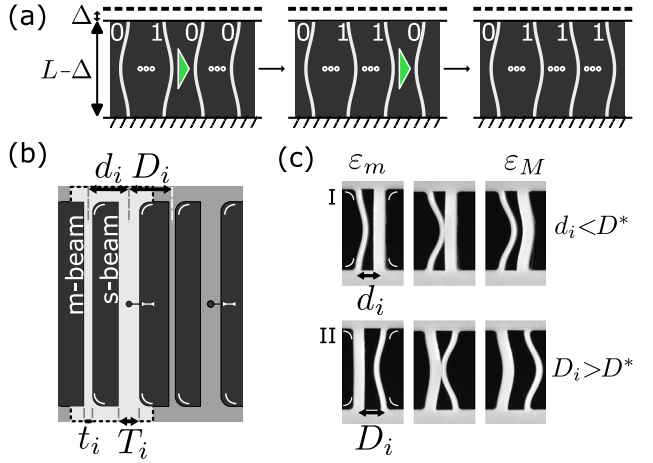

FIG. 1. (a) Schematic representation of the evolution of a "beam counter" metamaterial with $n = 4$ unit cells under two compression cycles. Each unit cell contains a buckled m-beam (memory beam) which encodes a single bit. When the strain $\varepsilon := \Delta/L$ is cycled between ε_m and ε_M, the m-beams interact (gray symbols), so that the "1" state is copied to the right (triangle), leading to the step wise advancing of the 1 state to the right. (b) Geometry of a unit cell i (highlighted), containing a slender m-beam of width t_i and a thicker, asymmetric a-beam (ancillary slitted beam) of width T_i. The lengths are nondimensionalized by setting the beams rest lengths to 1 (corners and slits highlighted by white markers). (c) Evolution of beam pairs under increased compression from ε_m (left) to ε_M (right): when the spacing d_i is smaller than a critical distance D^*, the buckled state of the slender beam is copied to the thick beam (top); when $D_i > D^*$, the buckled state of the thick beam is copied to the slender beam (bottom).

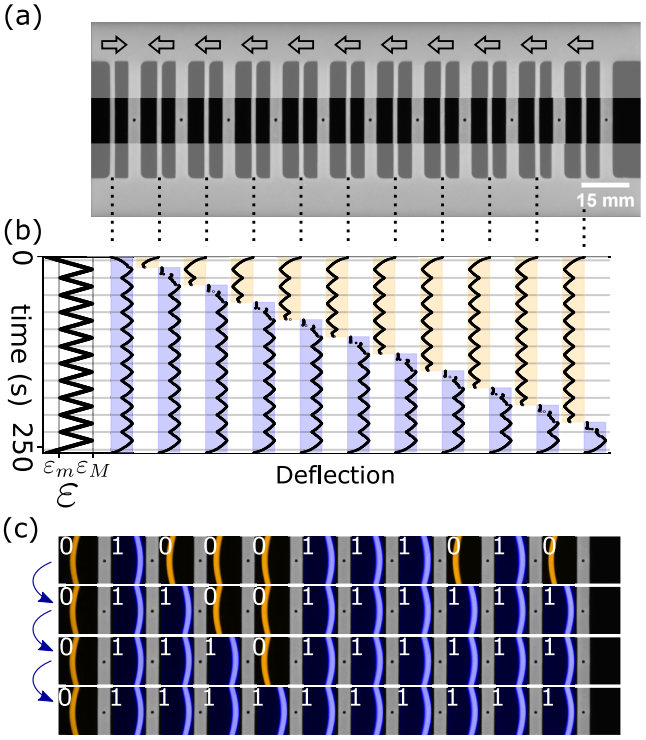

FIG. 2. (a) Beam counting metamaterial with 11 units, with center region highlighted; see movie 1 in [30] ($t_i = 0.040$, $T_i = 0.10$, $d_i = 0.13$, and $D_i = 0.15$). Arrows indicate weak symmetry breaking of the m-beams that makes the system reach state $\{10000000000\}$ when ε is increased from zero. (b) Space-time plot, tracing the center positions of each m-beam as a function of time under cyclic compression $\varepsilon_m \nearrow \varepsilon_M \searrow \varepsilon_m$ ($\varepsilon_m = 0.026$, $\varepsilon_M = 0.099$). Beams in state 0 (1) are highlighted in yellow (blue). (c) Evolution of the beam counter prepared in the initial state $\{01000111010\}$ (central parts shown only; beam state colored as above).

cycles, yet allows resetting the beam counter by momentarily cycling the strain towards zero. Second, the a-beams feature similarly rounded corners that makes them buckle left, and a slit which extends their reach when they snap to the right and the slit opens up [29]. As we show below, these symmetry breaking enhancements are crucial for their role in right-copying the 1 state of the m-beams. Third, we use the beam spacings d and D to control the interactions between a and m-beams. We found that when two buckled beams of unequal thickness are brought in contact, upon further compression they either both snap left or snap right—the direction depends on whether their distance is smaller or larger than a critical distance D^*. We choose $d_i < D^*$ and $D_i > D*$ so that contact interactions between neighboring m and a-beams favor rightward snapping of the beams [Fig. 1(c)].

Counting and transient memories.—We combine our unit cells to construct a beam counter with $n = 11$ unit cells, using standard 3D printing and molding techniques (see Supplemental Material [30]; Fig. 2). We cycle the compression in a custom built setup that allows accurate parallel compression of wide samples, and track the center locations of the middle of the m-beams [Fig. 2(b)]. Ramping up the strain from zero to ε_m, the system reaches the initial state $\{10000000000\}$ [Fig. 2(b)]. Repeated compression cycles show the step-by-step copying of the 1 state of the m-beams to the right, which involves rightward snapping of the appropriate m-beam just after ε has peaked [Fig. 2(b)]. Hence, the state evolves as $\{100\ldots0\} \to \{110\ldots0\} \to \ldots \to \{111\ldots1\}$ [Fig. 2(b)] (see Movie 1 in [30]). We characterize such "domain wall" states consisting of a string of 1's followed by 0's by the number of 0's, σ. The evolution of our beam counter under cyclic compression can thus be seen as counting down from $\sigma = 10$ to $\sigma = 0$. Our design is robust, can be scaled down, does not require disorder, and can be operated in a hand-held device (see movie 2 in [30]).

The evolution from the natural initial state $\{100\ldots\}$ only features a limited set of states, which do not contain substrings like 010 or 001. To demonstrate that our metamaterial correctly copies 1 bits to the right, we use manual manipulation to program the metamaterial in the initial state $\{01000111010\}$—this state contains all

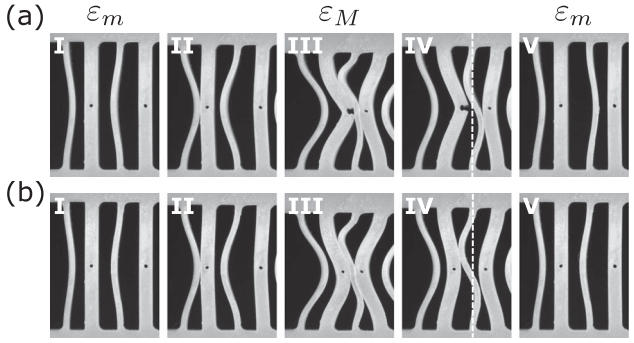

FIG. 3. Comparison of the evolution of two unit cells during a compression cycle. (a) Original design. (b) Design without slits, which does not copy the 1 state. Frames (aIV) and (bIV) are not at the same strain, but compare the states where the second m-beam just loses contact with one of its neighboring a-beams; note that the m-beam is then, respectively, to the right (a) and left (b) of the neutral line (dashed).

possible three-bit substrings. Its evolution shows that our metamaterial faithfully executes our target evolution [Fig. 2(c); see movie 3 in [30]). Moreover, we note that this initial state evolves to the absorbing state $\{11\ldots\}$ after only $\tau = 3$ cycles, as the largest numbers of 0's to the right of a 1 is equal to three. Here, the transient τ is not a material property but a simple function of the state [13,14].

A detailed inspection of the evolution of adjacent unit cells during their evolution illustrates that bit evolution takes place in two phases (Fig. 3). First, when ε is increased beyond a unit-cell dependent critical strain $\varepsilon^\dagger$, the 1 state of m_i is copied to a_i [Figs. 3(aI)–(aIII)]. During this first phase, the left a-beam snaps open to the right, and the m-beam becomes sandwiched between two a-beams [Fig. 3(aIII)]. In the second phase, ε is lowered to ε_m, and the sandwiched m-beam snaps right, after which all beams relax to their new configuration [Figs. 3(aIII)–3(aV)]. To illustrate how the slits facilitate the copying of the right-buckled state, we compare the sandwiched states for a-beams with and without slits [(Fig. 3); see movie 4 and Supplemental Material [30]]. Without slits, the sandwiched m-beam is pushed left and first loses contact with the right beam; with slits, the m-beam is pushed right, first loses contact with the left beam, and eventually moves right [Figs. 3(a) and 3(b)]. We stress that although the slits are essential in the current design, we also realized beam counting in an alternative design that does not feature slitted beams (see Movie 5 and Supplemental Material [30]).

Parallel counters and multiple transient memories.—By combining multiple beam counters with different values of $\varepsilon^\dagger$, we realize aggregate metamaterials which exhibit multiple transient memories. Specifically, we combine three $n = 4$ beam counters labeled aaa, bbb, and ccc which have respective critical thresholds $(\varepsilon_a^\dagger, \varepsilon_b^\dagger, \varepsilon_c^\dagger) \approx [0.073(4), 0.084(5), 0.092(2)]$ [Figs. 4(a) and 4(b)]. We label the resulting metamaterial as $aaa|bbb|ccc$, and characterize its state by the number of 0 beams in each counter, $\{\sigma_i\}$. We define driving cycles of different magnitude, A, B, C, as compression sweeps $\varepsilon_m \nearrow \varepsilon_M^{A,B,C} \searrow \varepsilon_m$, with $(\varepsilon_M^A, \varepsilon_M^B, \varepsilon_M^C) \approx (0.078, 0.089, 0.099)$, such that $\varepsilon_a^\dagger < \varepsilon_M^A < \varepsilon_b^\dagger < \varepsilon_M^B < \varepsilon_c^\dagger < \varepsilon_M^C$. Starting out in the initial state $\{\sigma_i\} = \{3, 3, 3\}$, a single driving cycle (A, B, or C) then advances one, two, or all three counters, yielding three distinct states $\{2, 3, 3\}$, $\{2, 2, 3\}$, or $\{2, 2, 2\}$, respectively. Hence, from the state we can uniquely infer the applied driving cycle. Crucially, longer driving sequences are also encoded in the internal state. We denote sequential driving cycles as, e.g., BAC, for which $\{\sigma_i\}$ evolves as $\{3, 3, 3\} \xrightarrow{B} \{2, 2, 3\} \xrightarrow{A} \{1, 2, 3\} \xrightarrow{C} \{0, 1, 2\}$ [Fig. 4(b)]. These states all encode specific information, e.g., state $\{1, 2, 3\}$ encodes one A and one B pulse, whereas $\{0, 1, 2\}$ encodes a memory of one B, one C and an arbitrary number of A pulses. The capacity of this aggregate metamaterial to count distinct signals can be enlarged by combining more counters or by increasing their length n. Finally, we stress that such metamaterials realize the Park Bench model for multiple transient memories [16,17].

Heterogeneity and sequential processing.—So far, the counting elements in our metamaterials all have the same threshold, and as a consequence, our metamaterials are insensitive to the order of input signals. However, combining unit cells with different thresholds realizes heterogeneous metamaterials whose response is sequence dependent and, e.g., discriminates driving cycles ABC from BAC. We realize the heterogeneous metamaterial bac [Figs. 4(c)–4(e)]. Starting from state $\sigma = 3$, we can use the same logic as before to infer its evolution and we subsequently collect all possible pathways in a transition graph [Fig. 4(c)]. This graph implies that the transient time τ depends on the driving magnitude, as driving cycles $AA\ldots$, $BB\ldots$, and $CC\ldots$ yield $\tau = 0$, 2, and 3, respectively. Moreover, we find that input BAC yields $\sigma = 0$ while all other three-character permutations of A, B, and C yield $\sigma = 1$ [Figs. 4(d) and 4(e)], illustrating the sequence dependent response of heterogenous counters.

Finally, by combining heterogeneous and homogeneous counters we realize an aggregate metamaterial that unambiguously detect a specific input "key" string and thus act as a sequential "lock." We note that state $\sigma = 0$ for counter bac is not unique to input BAC, but can also be reached with input sequences such as BBC and CCC [Fig. 4(c)]. Hence, to uniquely recognize a string BAC, we combine the counting metamaterial $aaa|bbb|ccc$ with the heterogeneous counter bac [Figs. 4(b) and 4(d)]. Out of all three-character strings, BAC is the only one that yields the collective state $\{\sigma\} = \{0, 1, 2, 0\}$ [Fig. 4(f)]. The experimental demonstration of the response of he $aaa|bbb|ccc|bac$ machine to input BAC is shown in Figs. 4(b) and 4(d), which correspond to a single experimental run where all four counters were actuated

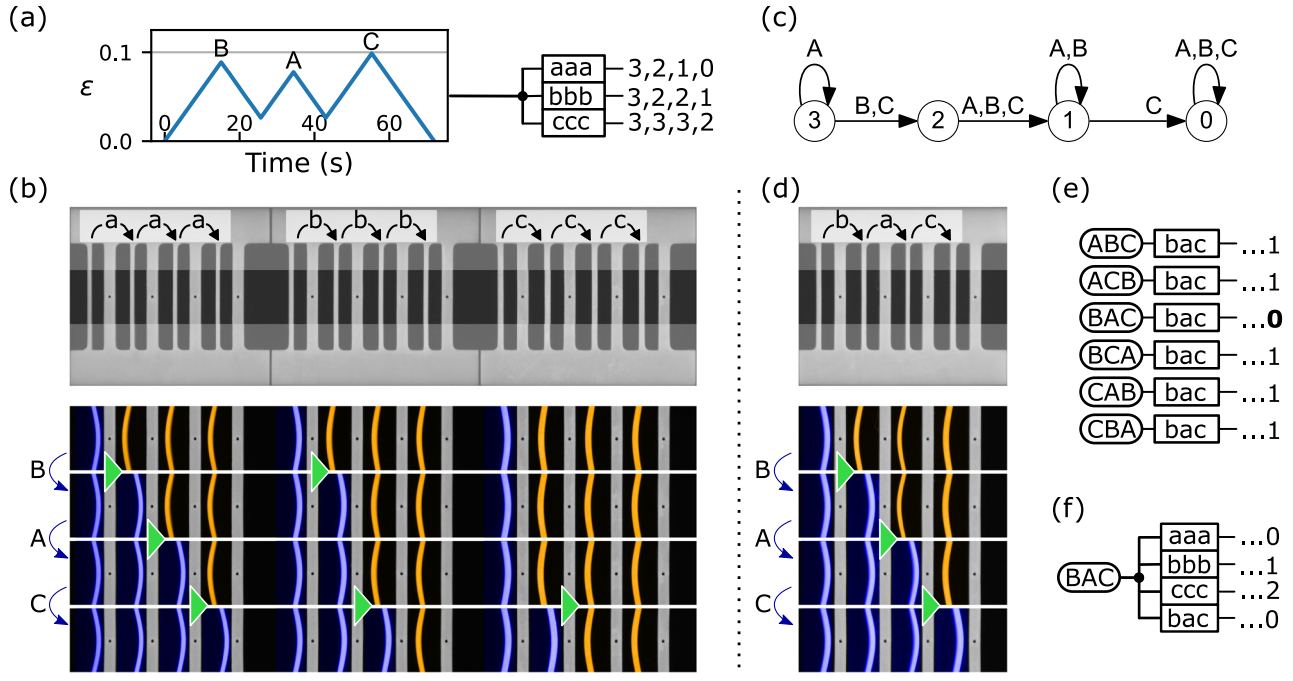

FIG. 4. Response of aggregate metamaterials containing multiple homogeneous and heterogeneous beam counters. (a) Complex driving cycles can be encoded as an input string (here *BAC*) and produce different sequential response in counters *aaa*, *bbb*, and *ccc* (boxes represent individual counters and numbers represent the sequence of states σ_i). (b) Experimental realization of the $aaa|bbb|ccc$ aggregate metamaterial, and snapshots of its pathway in response to input driving *BAC* (triangles highlight the right copying of a 1-bit). Note that t_i, d_i, and D_i subtly vary along the counters while T_i remains constant (see Supplemental Material [30]). The color and triangle overlay help to indicate the state and the transitions of the beams. (c) Transition graph of the heterogeneous counter *bac*. (d) Experimental realization and evolution of *bac* counter during input string *BAC* [panel (b) and (d) are snapshots of the same experiment]. (e) The output of the *bac* counter to all input sequences which are permutations of *ABC* (rounded boxes). (f) The four counters *aaa*, *bbb*, *ccc*, and *bac* operated in parallel reach the unique state $\{0120\}$ only for input sequence *BAC*. The homogeneous counters store the count of each signal, while the heterogeneous counter is sensitive to the specific permutation.

in parallel (see movie 6 in [30]). We note that our strategy can trivially be extended to longer sequences or larger alphabets.

While the design above cannot distinguish input *BAC* from longer sequences such as *ABAC*, we can detect such longer strings by extending the counter for the weakest signal: out of all possible input sequences, the metamaterial $aaaa|bbb|ccc|bac$ only reaches state $\{0, 1, 2, 0\}$ for input *BAC*, thus allowing to uniquely filter and detect such a string. Finally we note that designs featuring one heterogenous with multiple homogeneous counters are not optimal. Unique detection of, e.g., three symbol sequences with less than four counters can be achieved; in addition, many machines recognize multiple distinct input sequences (see Supplemental Material [30]).

Discussion and Outlook.—Our (aggregate) metamaterials provide a platform to realize (multiple) transient memories without disorder. By controlling heterogeneity, our results suggest that systematic explorations of driving protocols may reveal complex memory effects in disordered systems with driving-dependent transient times and sequence dependent responses. Moreover, our realization of multiple transient memories suggests that local regions, acting as independent transient counters, lead to multiple transient memories in extended disordered media. An intriguing question is which new memory effects emerge and which are washed out when the system size or degree of disorder is gradually increased.

From the perspective of information processing, our platform allows us to realize metamaterials with predictable countinglike pathways and easily readable internal states under cyclical driving. These metamaterials act as a sequential thresholding devices, and can be generalized to detect more driving magnitudes and longer sequences. Moreover, similar sequential behavior can be realized in other designs, e.g., without slits. In contrast to recent mechanical platforms that store mechanical bits [19] and perform Boolean logic [21,23], our metamaterials perform sequential computations, which are much more powerful than combinational logic. Extending our update rules to more complex cases, including those where the new state depends on multiple neighbors, including in higher dimensions, opens routes to create systems that are Turing complete, such as "rule 110" or Conway's game of life [20,31]. Such "cellular automata materials" would allow massively parallel computations *in materia*.

We thank H. Bense, M. Caelen, C. Coulais, D. Holmes, B. Durà Faulí, D. Kraft, C. Meulblok, and M. Munck for fruitful discussions and J. Mesman for technical support.

[1] D. J. Amit, Neural networks counting chimes, Proc. Natl. Acad. Sci. U.S.A. **85**, 2141 (1988).
[2] J. Böhm *et al.*, The venus flytrap dionaea muscipula counts prey-induced action potentials to induce sodium uptake, Curr. Bio. **26**, 286 (2016).
[3] M. Mungan, S. Sastry, K. Dahmen, and I. Regev, Networks and Hierarchies: How Amorphous Materials Learn to Remember, Phys. Rev. Lett. **123**, 178002 (2019).
[4] N. C. Keim, J. D. Paulsen, Z. Zeravcic, S. Sastry, and S. R. Nagel, Memory formation in matter, Rev. Mod. Phys. **91**, 035002 (2019).
[5] I. Regev, T. Lookman, and C. Reichhardt, Onset of irreversibility and chaos in amorphous solids under periodic shear, Phys. Rev. E **88**, 062401 (2013).
[6] C. F. Schreck, R. S. Hoy, M. D. Shattuck, and C. S. O'Hern, Particle-scale reversibility in athermal particulate media below jamming. Phys. Rev. E **88**, 052205 (2013).
[7] J. R. Royer and P. M. Chaikin, Precisely cyclic sand: Self-organization of periodically sheared frictional grains, Proc. Natl. Acad. Sci. U.S.A. **112**, 49 (2015).
[8] T. Kawasaki and L. Berthier, Macroscopic yielding in jammed solids is accompanied by a nonequilibrium first-order transition in particle trajectories, Phys. Rev. E **94**, 022615 (2016).
[9] M. O. Lavrentovich, A. J. Liu, and S. R. Nagel, Period proliferation in periodic states in cyclically sheared jammed solids, Phys. Rev. E **96**, 020101(R) (2017).
[10] K. Nagasawa, K. Miyazaki, and T. Kawasaki, Classification of the reversible-irreversible transitions in particle trajectories across the jamming transition point, Soft Matter **15**, 7557 (2019).
[11] W. Yeh, M. Ozawa, K. Miyazaki, T. Kawasaki, and L. Berthier, Glass Stability Changes the Nature of Yielding under Oscillatory Shear, Phys. Rev. Lett. **124**, 225502 (2020).
[12] N. C. Keim and J. D. Paulsen, Multiperiodic orbits from interacting soft spots in cyclically sheared amorphous solids, Sci. Adv. **7**, 7685 (2021).
[13] C. W. Lindeman and S. R. Nagel, Multiple memory formation in glassy landscapes, Sci. Adv. **7**, 7133 (2021).
[14] H. Bense and M. van Hecke, Complex pathways and memory in compressed corrugated sheets, Proc. Natl. Acad. Sci. U.S.A. **118**, e2111436118 (2021).
[15] D. Shohat, D. Hexner, and Y. Lahini, Memory from coupled instabilities in unfolded crumpled sheets, Proc. Natl. Acad. Sci. U.S.A. **119**, e2200028119 (2022).
[16] J. D. Paulsen, N. C. Keim, and S. R. Nagel, Multiple Transient Memories in Experiments on Sheared Non-Brownian Suspensions, Phys. Rev. Lett. **113**, 068301 (2014).
[17] J. D. Paulsen and N. C. Keim, Minimal descriptions of cyclic memories, Proc. R. Soc. A **475**, 20180874 (2019).
[18] K. Bertoldi, V. Vitelli, J. Christensen, and M. van Hecke, Flexible mechanical metamaterials, Nat. Rev. Mater. **2**, 1 (2017).
[19] T. Chen, M. Pauly, and P. M. Reis, A reprogrammable mechanical metamaterial with stable memory, Nature (London) **589**, 386 (2021).
[20] S. Wolfram, *Cellular Automata and Complexity: Collected Papers* (CRC Press, Boca Raton, 2018).
[21] H. Yasuda, P. R. Buskohl, A. Gillman, T. D. Murphey, S. Stepney, R. A. Vaia, and J. R. Raney, Mechanical computing, Nature (London) **598**, 39 (2021).
[22] C. Kaspar, B. J. Ravoo, W. G. van der Wiel, S. V. Wegner, and W. H. P. Pernice, The rise of intelligent matter, Nature (London) **594**, 345 (2021).
[23] C. El Helou, B. Grossmann, C. E. Tabor P. R. Buskohl, and R. L. Harne, Mechanical integrated circuit materials, Nature (London) **608**, 699 (2022).
[24] J. T. B. Overvelde, T. Kloek, J. J. A. D'haen, and K. Bertoldi, Amplifying the response of soft actuators by harnessing snap-through instabilities, Proc. Natl. Acad. Sci. U.S.A. **112**, 10863 (2015).
[25] C. Coulais, A. Sabbadini, F. Vink, and M. van Hecke, Multi-step self-guided pathways for shape-changing metamaterials, Nature (London) **561**, 512 (2018).
[26] M. Stern, V. Jayaram, and A. Murugan, Shaping the topology of folding pathways in mechanical systems, Nat. Commun. **9**, 4303 (2018).
[27] T. Jules, A. Reid, K. E. Daniels, M. Mungan, and F. Lechenault, The delicate memory structure of coupled origami switches, Phys. Rev. Res. **4**, 013128 (2022).
[28] D. Melancon, A. Elia Forte, L. M. Kamp, B. Gorissen, and K. Bertoldi, Inflatable origami: Multimodal deformation via multistability, Adv. Funct. Mater. **32**, 2201891 (2022).
[29] B. Durà Faulí, L. J. Kwakernaak, and M. van Hecke (to be published).
[30] See Supplemental Material at http://link.aps.org/supplemental/10.1103/PhysRevLett.130.268204 for details on sample fabrication and setup, alternative designs, evolution of the beam shapes during compression cycles, design parameters, heterogeneous metamaterials, and movies.
[31] M. Gardner, The fantastic combinations of John Conway's new solitaire game "life," Sci. Am. **223**, 120 (1970).